Optical spectroscopy and frequency upconversion properties of Tm 3+ doped tungstate fluorophosphate glasses

Gaël Poirier, Vladimir A. Jerez, Cid B. de Araújo, Younes Messaddeq, Sidney J. L. Ribeiro, and Marcel Poulain

Citation: Journal of Applied Physics **93**, 1493 (2003); doi: 10.1063/1.1536017
View online: http://dx.doi.org/10.1063/1.1536017
View Table of Contents: http://scitation.aip.org/content/aip/journal/jap/93/3?ver=pdfcov
Published by the AIP Publishing

Optical spectroscopy and frequency upconversion properties of Tm^{3+} doped tungstate fluorophosphate glasses

Gaël Poirier
Instituto de Química, UNESP, CP 355, CEP 14801-970, Araraquara, SP, Brazil and Laboratoire des Matériaux Photoniques, Bât 10B, Campus de Beaulieu, Université de Rennes I, Rennes, France

Vladimir A. Jerez and Cid B. de Araújo[a)]
Departamento de Física, Universidade Federal de Pernambuco, 50670-901 Recife, PE, Brazil

Younes Messaddeq and Sidney J. L. Ribeiro
Instituto de Química, UNESP, CP 355, CEP 14801-970, Araraquara, SP, Brazil

Marcel Poulain
Laboratoire des Matériaux Photoniques, Bât 10B, Campus de Beaulieu, Université de Rennes I, Rennes, France

(Received 9 September 2002; accepted 14 November 2002)

Tungstate fluorophosphate glasses of good optical quality were synthesized by fusion of the components and casting under air atmosphere. The absorption spectra from near-infrared to visible were obtained and the Judd–Ofelt parameters determined from the absorption bands. Transition probabilities, excited state lifetimes and transition branching ratios were determined from the measurements. Pumping with a 354.7 nm beam from a pulsed laser resulted in emission at 450 nm due to transition $^1D_2 \rightarrow {}^3F_4$ in Tm^{3+} ions and a broadband emission centered at ≈550 nm attributed to the glass matrix. When pumping at 650 nm, two emission bands at 450 nm ($^1D_2 \rightarrow {}^3F_4$) and at 790 nm ($^3H_4 \rightarrow {}^3H_6$) were observed. Excitation spectra were also obtained in order to understand the origin of both emissions. Theoretical and experimental lifetimes were determined and the results were explained in terms of multiphonon relaxation. © *2003 American Institute of Physics.*
[DOI: 10.1063/1.1536017]

I. INTRODUCTION

Thulium ion (Tm^{3+}) has been recognized as one of the most efficient rare-earth (RE) ions for obtaining laser emission, frequency upconversion, as well as to be used in optical amplifiers, when doping different hosts.[1–5] Laser emission and amplified spontaneous emission studies have been reported in crystals, bulk glasses, and optical fibers doped with Tm^{3+}.[1–3] Frequency upconversion in a variety of Tm^{3+} doped materials was also investigated in the past.[6–13] Of particular interest is the possibility of obtaining strong blue emission from Tm^{3+} doped materials pumped in the red and in the infrared. Upconversion laser emission and amplified spontaneous emission studies have been reported for Tm^{3+} doped optical fibers and channel waveguides.[1,2,12,13]

Recently a number of reports became available where detailed spectroscopic properties of Tm^{3+} were analyzed in glasses such as fluorozirconate,[14,15] fluoroindate,[16–18] fluorophosphate,[19,20] fluoroindogallate,[21] and silicate.[22] Each glass host presents certain characteristics that favor specific applications. In particular, fluorophosphate glasses have been recently investigated because of their potential as a laser host material and optical amplifier.[19,23–25]

In this work, tungstate fluorophosphate glasses have been chosen as host matrices to study the spectroscopic properties of Tm^{3+}. Two previous articles report some of the physical properties of these glasses.[26,27] In Ref. 26 physical properties were investigated with respect to chemical composition. Density, refractive index, and characteristic temperatures were measured. The Raman spectra of this glass allowed us to conclude that the vitreous network is formed by WO_4, PO_4 and PO_3F tetrahedra with a variable number of nonbridging atoms. Nonlinear absorption measurements, performed at 660 nm,[27] have shown that these glasses can be used for optical limiting due to the large two-photon absorption coefficient. Their performance can be controlled by adjusting the tungsten oxide concentration.

The present work includes the investigation of one-photon absorption and emission spectroscopy, lifetime measurements and the study of red-to-blue upconversion processes. We first deduced the Judd–Ofelt parameters from the absorption spectra to access theoretical spectroscopic quantities such as transition probabilities, branching ratios, and radiative lifetimes. Further the samples were excited by 354.7 or 650 nm laser light producing emissions that were analyzed according to its spectrum and time evolution. The theoretical and experimental level lifetimes measured were understood considering radiative relaxation, multiphonon decay, and energy transfer among Tm^{3+} ions. A mechanism is also proposed to describe the origin of the upconversion process observed.

[a)]Author to whom correspondence should be addressed; electronic mail: cid@df.ufpe.br

II. EXPERIMENTAL AND THEORETICAL BACKGROUND

A. Experiment

The glass samples studied have the following compositions in mol %: $(48-x)NaPO_3-12\ BaF_2-40\ WO_3-xTmF_3$, where $x=0$; 0.2; 0.4; 0.6; 0.8; 1.0. TmF_3 was synthesized by fluoration of Tm_2O_3 at 400 °C for 2 h with ammonium bifluoride NH_4F, HF in a platinum crucible. Then the excess was volatilized at 500 °C for 1 h. All components were mixed and melted in air atmosphere at 1000 °C for 1 h in a platinum crucible. The melt was then casted in a mold preheated near the transition temperature (415 °C) and treated at this temperature for 2 h in order to remove mechanical stress. Large samples of good optical quality were prepared.

Absorption spectra were obtained using a spectrophotometer operating from 200 to 3000 nm. The study of excited states was performed using a Nd:yttrium–aluminum–garnet (YAG) laser, which produces 10 ns pulses with a repetition rate of 5 Hz. For excitation at 354.7 nm the third harmonic of the laser light was generated using a potassium dihydrogen phosphate crystal. For the experiments in the visible range a Nd:YAG pumped dye laser operating from 608 to 682 nm was used.

The fluorescence emission was dispersed using a 0.50 m spectrometer, with a resolution of 5 Å, coupled to a photomultiplier. The signals were recorded using a digital storage oscilloscope connected to a computer. All data were taken at room temperature.

B. Theoretical background

The features normally observed in the absorption spectra of a RE ion are $4f$-$4f$ transitions. In the theory of a free RE ion, these transitions are forbidden because they would connect states having the same parity, but in the solid state the influence of the crystalline field on the RE ion allows such $4f$ transitions. Most of the $4f$-$4f$ transitions are induced electric dipole transitions and usually magnetic dipole transitions can be neglected.[1,2,4] The intensity of an absorption band can be evaluated by the dipole strength P which is determined using the relation[28]

$$P=\frac{2303mc^2}{N\pi e^2}\int \varepsilon_i(\sigma)d(\sigma)=4.32\times10^{-9}\times A, \qquad (1)$$

where m is the electron mass, c the speed of light, N the Avogadro number, and e the electron charge. A is the integrated absorption associated with the considered transition.

According to the Judd–Ofelt theory[29,30] from the standard $4f$-$4f$ intensity model, the oscillator strength of a transition between two multiplets aJ and bJ' is given by

$$P=\frac{8\pi^2 m\nu}{3h(2J+1)}\chi_a\sum_{\lambda=2,4,6}\Omega_\lambda|\langle aJ'\|U^\lambda\|bJ\rangle|^2, \qquad (2)$$

where ν is the mean frequency between the two levels (in cm^{-1}), $\chi_a=(n^2+2)^2/9n$ is the Lorentz local field correction for the absorption (n being the refractive index of the medium), U^λ is a unit operator of rank λ and Ω_λ are the Judd–Ofelt intensity parameters. The Ω_λ parameters can be determined using the P values obtained using Eqs. (1) and (2). The term inside the squared modulus is the reduced matrix element.[29–31]

TABLE I. Chemical compositions of the glasses studied in this work.

Sample	Chemical composition (mol %)			
	$NaPO_3$	BaF_2	WO_3	TmF_3
NBWT2	47.8	12	40	0.2
NBWT4	47.6	12	40	0.4
NBWT6	47.4	12	40	0.6
NBWT8	47.2	12	40	0.8
NBWT10	47	12	40	1.0

The probability of radiative emission between the aJ and bJ' levels is given by

$$A_{JJ'}=\frac{64\pi^4\nu^3e^2}{3h(2J+1)c^3}\chi_e\sum_{\lambda=2,4,6}\Omega_\lambda|\langle aJ\|U^\lambda\|bJ'\rangle|^2, \qquad (3)$$

where $\chi_e=n(n^2+2)^2/9$ is the effective field correction for emission at a well-localized center in a medium of isotropic refractive index n, h is the Planck's constant and e is the electron charge. $A_{JJ'}$ is related to the radiative lifetime τ_R of an excited state by

$$\tau_R=\frac{1}{\Sigma_{J'}A_{JJ'}} \qquad (4)$$

and the branching ratio $\beta_{JJ'}$, corresponding to the emission from an excited level J to J', is

$$\beta_{JJ'}=\frac{A_{JJ'}}{\Sigma_{J'}A_{JJ'}}. \qquad (5)$$

III. RESULTS AND DISCUSSION

The experiments were performed using tungstate fluorophosphate glass samples containing different Tm^{3+} concentrations with matrix composition as presented in Table I.

A. Absorption measurements

The absorption spectrum of the NBWT10 glass is presented in Fig. 1 where the absorption bands are attributed to transitions from the ground state ($^3H_6$) to excited states of

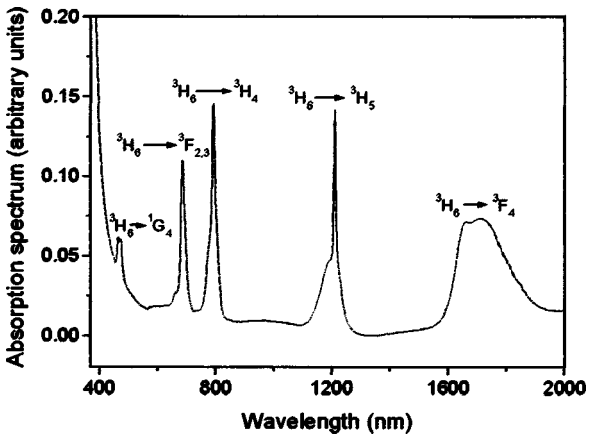

FIG. 1. Absorption spectrum of the NBWT10 glass sample.

TABLE II. Oscillator strengths and intensity parameters.

Transitions	Energy (cm^{-1})	P_{EXP}	P_{THEO}
$^3H_6 \rightarrow {}^3F_4$	5835	2.28×10^{-6}	2.61×10^{-6}
$^3H_6 \rightarrow {}^3H_5$	8283	1.65×10^{-6}	1.47×10^{-6}
$^3H_6 \rightarrow {}^3H_4$	12 640	2.78×10^{-6}	3.05×10^{-6}
$^3H_6 \rightarrow {}^3F_{2,3}$	14 575	2.44×10^{-6}	2.57×10^{-6}
$^3H_6 \rightarrow {}^1G_4$	21 276	8.40×10^{-7}	7.48×10^{-7}
$^3H_6 \rightarrow {}^1D_2$	28 050	...	6.53×10^{-7}
$\Omega_2 = 5.28\times10^{-20}$ cm^2; $\Omega_4 = 2.32\times10^{-21}$ cm^2; $\Omega_6 = 1.16\times10^{-20}$ cm^2			

the Tm^{3+} ion. The absorption band corresponding to the $^1D_2$ level cannot be observed in the spectrum because the band gap energy of the glass matrix is smaller than the energy of the transition between the $^3H_6$ and $^1D_2$ levels. It was observed that the amplitude of the bands decreases for lower Tm^{3+} concentrations but their spectral position does not change. From the absorption bands, we calculated the experimental oscillator strengths using Eq. (1) and then determined the Ω_λ intensity parameters as described in Sec. II B.

Table II presents the experimental and theoretical oscillator strengths together with the intensity parameters obtained. For the $^3H_6 \rightarrow {}^1D_2$ transition, we estimated a transition energy of 28 050 cm^{-1}. The values reported in Table II were used to calculate the spectroscopic parameters with basis on the Judd–Ofelt theory.

Table III gives the energy of possible $J \rightarrow J'$ transitions for the NBWT10 glass. The quantities $A_{JJ'}$, τ_R and $\beta_{JJ'}$ were calculated using Eqs. (3), (5), and (6), respectively, and the results are included in Table III.

TABLE III. Values of the energy gap ΔE, transition probabilities $A_{JJ'}$, branching ratios, $\beta_{JJ'}$, between multiplets J and J', and radiative lifetime, τ_R, for each excited state.

Transitions		ΔE (cm^{-1})	$A_{JJ'}$	$\beta_{JJ'}$	τ_R (μs)
$^3F_4 \rightarrow$	$^3H_6$	5835	248.24	1	4028
$^3H_5 \rightarrow$	$^3F_4$	2448	6.94	0.029	4203
	$^3H_6$	8283	231	0.970	
$^3H_4 \rightarrow$	$^3H_5$	4357	5.75	0.003	642
	$^3F_4$	6805	109.13	0.070	
	$^3H_6$	12 640	1441.65	0.926	
$^3F_3 \rightarrow$	$^3H_4$	1948	2.92	0.001	501
	$^3H_5$	6305	399.91	0.200	
	$^3F_4$	8753	65.77	0.032	
	$^3H_6$	14 588	1527.96	0.765	
$^3F_2 \rightarrow$	$^3F_3$	587	0.0048	2.882	597
	$^3H_4$	2535	18.13	0.010	
	$^3H_5$	6892	87	0.051	
	$^3F_4$	9340	889.82	0.531	
	$^3H_6$	15 175	678.72	0.405	
$^1G_4 \rightarrow$	$^3F_2$	6101	7.49	0.003	454
	$^3F_3$	6688	44.43	0.020	
	$^3H_4$	8636	290.06	0.131	
	$^3H_5$	12 993	779.12	0.353	
	$^3F_4$	15 441	135.62	0.061	
	$^3H_6$	21 276	945.55	0.429	
$^1D_2 \rightarrow$	$^1G_4$	6774	215.78	0.007	34
	$^3F_2$	12 875	573.91	0.019	
	$^3F_3$	13 462	1412.38	0.048	
	$^3H_4$	15 410	2107.18	0.071	
	$^3H_5$	19 767	98.48	0.003	
	$^3F_4$	22 215	22 357.96	0.761	
	$^3H_6$	28 050	2598.12	0.088	

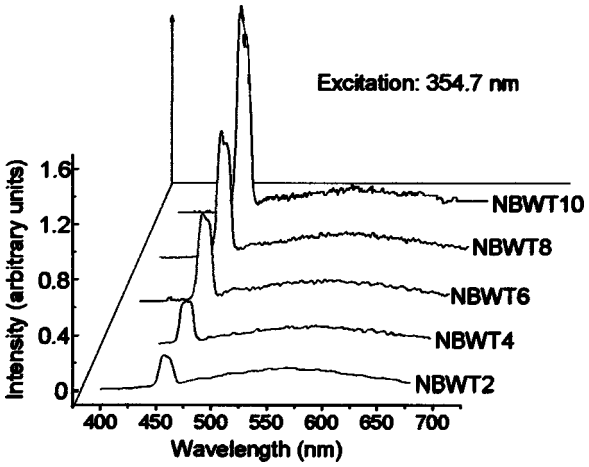

FIG. 2. Emission spectra for excitation at 354.7 nm.

B. Emission spectra

All samples were pumped by a 354.7 nm light beam which allows excitation of the $^1D_2$ level of the Tm^{3+} ion. The emission spectra obtained are shown in Fig. 2. Notice that only two emission bands are observed in the 350–700 nm range. The band centered at 450 nm is attributed to the $^1D_2 \rightarrow {}^3F_4$ transition of the Tm^{3+} ion because its intensity increases for increasing values of Tm^{3+} concentration.[15] The broad emission band centered around 550 nm is due to the glass matrix because it is observed when pure glass samples, without Tm^{3+}, are excited. This band is attributed to the transition from the conduction band to the valence band of the vitreous material because the gap between these two bands is $\approx$18 000 cm^{-1}.

Only one Tm^{3+} transition is observed when the $^1D_2$ level is excited, in agreement with the theoretical predictions based on the Judd–Ofelt theory. As can be seen in Table III, the transition probability between the states $^1D_2$ and $^3F_4$ is much higher than the others and the branching ratio of this transition is $\approx$0.76. In other words, the transition $^1D_2 \rightarrow {}^3F_4$ is the most probable transition. We note that similar behavior was reported for Tm^{3+} doped fluorophosphate glasses.[19]

The upconversion (UC) fluorescence spectra of Tm^{3+} doped samples for excitation at 650 nm are shown in Fig. 3. The UC emission at 450 nm is assigned to $^1D_2 \rightarrow {}^3F_4$ transition of Tm^{3+} and the down conversion fluorescence band at 790 nm is assigned to the $^3H_4 \rightarrow {}^3H_6$ transition.[15] The number of absorbed photons for each UC photon emitted was determined plotting the fluorescence intensity as a function of the laser intensity as shown in Fig. 4. The quadratic dependence indicates that two laser photons are necessary to generate each photon at 450 nm. The linear behavior of the signal emitted at 790 nm as a function of the laser intensity indicates a simple down conversion process.

Figure 5(a) shows the proposed pathway which leads to the 790 nm fluorescence. After absorption of one photon

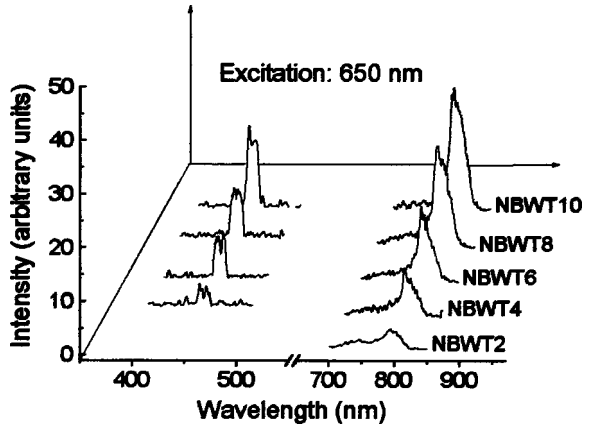

FIG. 3. Fluorescence spectra observed for excitation at 650 nm.

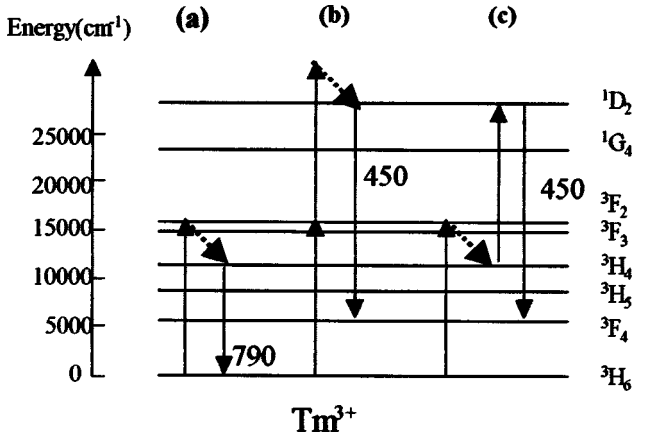

FIG. 5. Energy level diagram of Tm^{3+} and possible transition pathways in the experiments. Solid lines represent electric dipole transitions while dotted lines refer to nonradiative transitions.

from the incident laser beam, a nonradiative relaxation from state $^3F_3$ to state $^3H_4$ occurs. Afterwards, one photon with a wavelength of 790 nm is emitted. Figures 5(b) and 5(c) illustrate two possible pathways for the upconverted emission at 450 nm. In Fig. 5(b) a two-photon transition to the conduction band of the glass followed by nonradiative decay to state $^1D_2$ is represented. In Fig. 5(c) a two-photon stepwise absorption is considered to populate level $^1D_2$. In order to determine which route is dominant, we measured the excitation spectra of the emissions at 450 and at 790 nm which are plotted in Fig. 6. The emission at 790 nm is more efficient for excitation at ≈684 nm because the laser wavelength is resonant with transition $^3H_6 \rightarrow {}^3F_3$. On the other hand, the upconverted emission at 450 nm is more efficient for excitation at ≈657 nm. We note that the pathway shown in Fig. 5(b) would be more efficient for excitation at 684 nm than at 657 nm because of one-photon resonance with transition $^3H_4 \rightarrow {}^3F_3$ which has an absorption cross section larger than transition $^3H_6 \rightarrow {}^3F_2$. However, for the route shown in Fig. 5(c) the maximum efficiency at ≈657 nm is understood considering that the energy of photons at 680 nm is smaller than the energy gap between states $^3H_4$ and $^1D_2$ while for excitation at ≈657 nm both transitions $^3H_6 \rightarrow {}^3F_2$ and $^3H_4 \rightarrow {}^1D_2$ are resonant. Accordingly, we conclude that the pathway responsible for the frequency upconversion process is the one shown in Fig. 5(c).

C. Excited state lifetimes

The lifetime of an excited RE state in a glass matrix is governed by radiative and nonradiative processes. The nonradiative processes can be due to multiphonon relaxation or to energy transfer between the RE ions. The probability of multiphonon relaxation is larger for a glass matrix with large phonon energies while the energy transfer between RE ions increases by increasing the rare earth concentration. Hence, the lifetime of an excited state can be described by

$$\frac{1}{\tau} = \frac{1}{\tau_R} + W_{\mathrm{MP}} + W_{\mathrm{ET}}, \tag{6}$$

were τ is the actual lifetime, τ_R is the radiative lifetime, W_{MP} is the probability of relaxation due to multiphonon emission and W_{ET} is the probability of energy transfer among neighbor ions.

The lifetimes of the $^3H_4$ and $^1D_2$ levels were determined, under 650 nm excitation, measuring the decay rate of the emissions at 790 and 450 nm, respectively. The results given in Table IV show that τ and τ_R are very much different although the error estimated in the calculations of τ_R is ~20%. The discrepancy between τ and τ_R can only be understood considering that nonradiative processes dominate

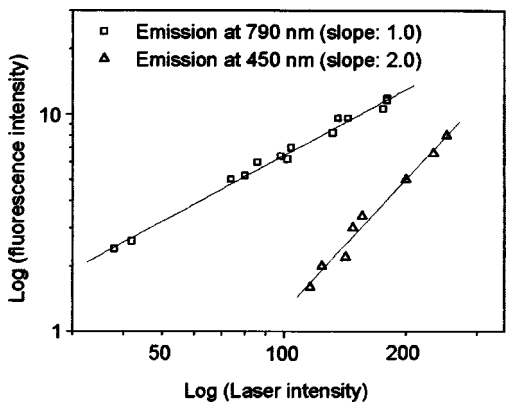

FIG. 4. Dependence of the 450 and 790 nm emission intensities on 650 nm excitation power.

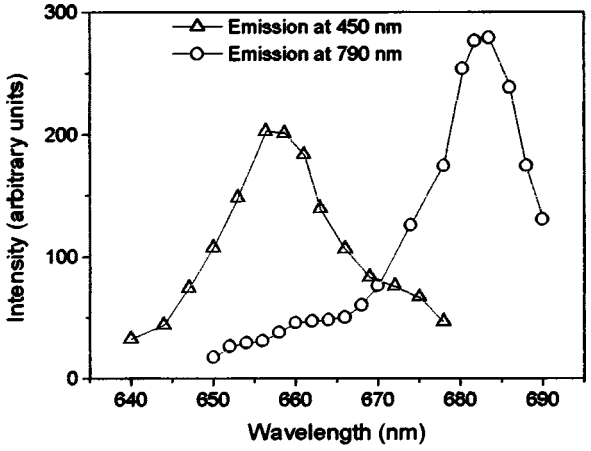

FIG. 6. Excitation spectra of the fluorescence bands at 450 and at 790 nm.

TABLE IV. Experimental and theoretical radiative lifetimes of the $^3H_4$ and $^1D_2$ levels.

	$^3H_4$ level	$^1D_2$ level
Theoretical radiative lifetime	642 μs	34 μs
Experimental lifetime		
Sample NBWT2	21±2.0 μs	4.7±2.0 μs
Sample NBWT4	21±2.0 μs	4.5±2.0 μs
Sample NBWT6	20±2.0 μs	4.6±2.0 μs
Sample NBWT8	19±2.0 μs	4.5±2.0 μs
Sample NBWT10	19±2.0 μs	4.3±2.0 μs

the lifetime of the levels. Since, as presented in Table IV, the lifetimes are not dependent on the Tm^{3+} concentration, we conclude that W_{ET} can be neglected and thus the actual lifetimes are due to multiphonon (MP) emission. In fact, MP relaxation is expected to be relevant because these tungstate glasses have large cutoff phonon energy ($\approx$940 cm^{-1}).[26] This interpretation allows us to determine the MP relaxation rate for $^3H_4$ and $^1D_2$ levels from Eq. (6) which gives $W_{MP}(^3H_4) = 48\,442\ s^{-1}$ and $W_{MP}(^1D_2) = 192\,810\ s^{-1}$. The value of $W_{MP}(^3H_4)$ is in agreement with estimates based in the *energy gap law* considering that the relaxation between $^3H_4$ and $^3H_5$ levels involves 4–5 phonons. The lifetime of level $^1D_2$ is small because it is positioned in the glass conduction band, which favors nonradiative relaxation.

IV. CONCLUSION

Spectroscopic properties of Tm^{3+} ions in tungstate fluorophosphate glasses were studied. When excited at 354.7 nm only one fluorescence band of Tm^{3+} at 450 nm, due to the $^1D_2 \rightarrow {}^3F_4$ transition, is observed. A broadband centered around 550 nm, corresponding to decay from the conduction band to the valence band of the glass matrix, was also detected. The excitation at $\approx$655 nm produced emission at 450 nm due to decay from $^1D_2$ to $^3F_4$ and emission at 790 nm corresponding to the $^3H_4 \rightarrow {}^3H_6$ transition. The excitation mechanisms involved in these processes were determined based on the excitation spectra. The results are in good agreement with predictions based on the Judd–Ofelt theory. No quenching mechanism was observed in the range of 0.2–1.0 mol % of Tm^{3+} as reported for other fluorophosphate glasses.[32] The lifetimes of the excited states of Tm^{3+} were found to be dominated by multiphonon relaxation.

ACKNOWLEDGMENTS

Financial support for this work by the Brazilian Conselho Nacional de Desenvolvimento Científico e Tecnológico-CNPq, Programa de Nucleos de Excelência-PRONEX/MCT (Brazil) and Conseil Régional de Bretagne (France) are gratefully acknowledged.

[1] See, for example, *Rare-Earth Doped Fiber Lasers and Amplifiers*, edited by M. J. F. Digonnet (Dekker, New York, 1993), and references therein.
[2] See, for instance, M. Yamane and Y. Asahara, *Glasses for Photonics* (Cambridge University Press, Cambridge, UK, 2000).
[3] J. Y. Allain, M. Monerie, and H. Poignant, Electron. Lett. **26**, 166 (1990).
[4] See, for example, R. Reisfeld and C. K. Jorgensen, *Lasers and Excited States of Rare-Earth* (Springer, New York, 1977).
[5] K. Hirao, S. Tanabe, S. Kishimoto, K. Tamai, and N. Soga, J. Non-Cryst. Solids **135**, 90 (1991).
[6] D. C. Yeh, R. R. Petrin, W. A. Sibley, V. Madigou, J. L. Adam, and M. J. Suscavage, Phys. Rev. B **39**, 80 (1989).
[7] A. Brenier, R. Moncorge, and C. Pedrini, IEEE J. Quantum Electron. **26**, 967 (1990).
[8] S. Tanabe, K. Tamai, K. Hirao, and N. Soga, Phys. Rev. B **47**, 2507 (1993).
[9] L. B. Shaw, R. S. F. Chang, and N. Djeu, Phys. Rev. B **50**, 6609 (1994).
[10] E. W. J. L. Oomen, J. Lumin. **50**, 317 (1992).
[11] K. Hirao, S. Todoroki, and N. Soga, J. Non-Cryst. Solids **143**, 40 (1992).
[12] A. S. L. Gomes, C. B. de Araújo, B. J. Ainslie, and S. P. Craig-Ryan, Appl. Phys. Lett. **57**, 2169 (1990).
[13] J. R. Bonar, M. V. D. Vermelho, A. J. Mc Laughlin, P. V. S. Marques, J. S. Aitchson, A. G. Bezerra, Jr., J. F. Martins-Filho, A. S. L. Gomes, and C. B. de Araújo, Opt. Commun. **141**, 137 (1997).
[14] R. S. Quimby, J. Appl. Phys. **90**, 1683 (2001).
[15] W. Tian and B. R. Reddy, Opt. Lett. **26**, 1580 (2001).
[16] S. Kishimoto and K. Hirao, J. Appl. Phys. **80**, 1965 (1996).
[17] I. R. Martin, V. D. Rodriguez, R. Alcalá, and R. Cases, J. Non-Cryst. Solids **161**, 294 (1993).
[18] C. B. de Araújo, G. S. Maciel, L. de S. Menezes, N. Rakov, E. L. Falcão Filho, V. A. Jerez, and Y. Messaddeq, *Frequency Upconversion in Rare-Earth Doped Fluoroindate Glasses* (to be published).
[19] K. Binnemans, R. Van Deun, C. Görller-Walrand, and J. L. Adam, J. Non-Cryst. Solids **238**, 11 (1998).
[20] G. Ozen, A. Kermaoui, J. P. Denis, W. Xu, F. Pelle, and B. Blanzat, J. Lumin. **63**, 85 (1995).
[21] K. Miazato, D. F. de Souza, A. Delben, J. R. Delben, S. L. de Oliveira, and L. A. O. Nunes, J. Non-Cryst. Solids **273**, 246 (2000).
[22] A. P. Otto, K. S. Brewer, and A. J. Silversmith, J. Non-Cryst. Solids **265**, 176 (2000).
[23] R. Balda, J. Fernández, A. de Pablos, J. M. F. dez-Navarro, and M. A. Arriandiaga, Phys. Rev. B **53**, 5181 (1996).
[24] R. Balda, J. Fernández, and A. de Pablos, J. Phys. IV **C4**, 509 (1994).
[25] R. Van Deun, K. Binnemans, C. Görller-Walrand, and J. L. Adam, J. Alloys Compd. **283**, 59 (1999).
[26] G. Poirier, Y. Messaddeq, S. J. L. Ribeiro, and M. Poulain, J. Non-Cryst. Solids (to be published).
[27] G. Poirier, C. B. de Araújo, Y. Messaddeq, S. J. L. Ribeiro, and M. Poulain, J. Appl. Phys. **91**, 10221 (2002).
[28] W. T. Carnall, *Handbook of Phys. Chem. Rare Earths* (North-Holland, Amsterdam, 1979).
[29] B. R. Judd, Phys. Rev. **127**, 750 (1962).
[30] G. S. Ofelt, J. Chem. Phys. **37**, 511 (1962).
[31] W. T. Carnall, H. Crosswhite, and H. M. Crosswhite, Report, 1977.
[32] X. Zou and H. Toratani, J. Non-Cryst. Solids **195**, 113 (1996).